

Location-Based Beamforming and Physical Layer Security in Rician Wiretap Channels

Chenxi Liu, *Student Member, IEEE*, and Robert Malaney, *Member, IEEE*

Abstract—We propose a new location-based beamforming (LBB) scheme for wiretap channels, where a multi-antenna source communicates with a single-antenna legitimate receiver in the presence of a multi-antenna eavesdropper. We assume that all channels are in a Rician fading environment, the channel state information from the legitimate receiver is perfectly known at the source, and that the only information on the eavesdropper available at the source is her location. We first describe how the optimal beamforming vector that minimizes the secrecy outage probability of the system is obtained, illustrating its dependence on the eavesdropper's location. We then derive an easy-to-compute expression for the secrecy outage probability when our proposed LBB scheme is adopted. We also consider the positive impact a friendly jammer can have on our beamforming solution, showing how the path to optimality remains the same. Finally, we investigate the impact of location uncertainty on the secrecy outage probability, showing how our solution can still allow for secrecy even when the source only has a noisy estimate of the eavesdropper's location. Our work demonstrates how a multi-antenna array, operating in the most general channel conditions and most likely system set-up, can be configured rapidly in the field so as to deliver an optimal physical layer security solution.

Index Terms—Physical layer security, wiretap channel, Rician fading, secrecy outage, jamming.

I. INTRODUCTION

PHYSICAL layer security has attracted significant research attention recently. Compared to the traditional upper-layer cryptographic techniques using secret keys, physical layer security safeguards wireless communications by directly exploiting the randomness offered by wireless channels without using secret keys, and thus has been recognized as an alternative for cryptographic techniques [1]. The principle of physical layer security was first studied in [2] assuming single-input single-output systems. It was shown that secrecy can only exist when the wiretap channel between the source and the eavesdropper is a degraded version of the main channel between the source and the legitimate receiver. Subsequently, this result was generalized to the case where the main channel and the wiretap channel are independent [3].

More recently, implementing multi-input multi-output (MIMO) techniques at the source/legitimate receiver has been shown to significantly improve the physical layer security of wiretap channels [4–14]. In terms of MIMO techniques, beamforming [4–9], artificial noise [10–12], and transmit antenna

selection [13, 14] are just a few techniques that can be utilized to boost the physical layer security of wiretap channels. In [4–14], it is assumed that the channel state information (CSI) from the eavesdropper is perfectly or statistically known at the source. This assumption, however, is unlikely to be valid in practice - especially when the eavesdropper is not an authorized component of the communication system.

In this paper we propose a location-based beamforming (LBB) scheme that does not require any form of CSI be passed by the eavesdropper back to the source. Rather, we will assume that some *a priori* known location information of the eavesdropper is available to the source. Such a scenario can occur in many circumstances, such as those detailed in [15]. In our scheme, we assume that *all* of the communication channels are in a Rician fading environment. That is, *all* the channels can vary from pure line-of-sight (LOS) channel to pure Rayleigh channel as the Rician K -factors in the channels change. We also assume that the CSI from the legitimate receiver is *perfectly* known at the source, while the *only* information on the eavesdropper available at the source is her location¹. Our key goal is to determine the beamforming vector at the source that minimizes the secrecy outage probability of the system, given the CSI of the main channel and the eavesdropper's location.

Perhaps the most relevant works to ours are those of [15] and [16]. In [15], the secrecy outage probability of a LBB scheme in Rician wiretap channels was investigated under the assumption that no CSI from the legitimate receiver was available. In [16], the secrecy outage probability was examined in Rician wiretap channels where the source is equipped with a large number of antennas. Different from [15] and [16], we propose a new LBB scheme utilizing the CSI from the legitimate receiver and the eavesdropper's location. We note that use of the CSI from the legitimate receiver will naturally lead to a reduction in the secrecy outage probability, but (more importantly) it will also enable us to determine the optimal beamforming vector at the source in a new and much more efficient manner. Moreover, we introduce a jammer to the system. Our contributions are summarized as follows:

- We derive a simple expression of the secrecy outage probability when the eavesdropper's location and the CSI of the main channel are known. We highlight that our expression is valid for arbitrary values of signal-to-noise ratios (SNR) and Rician K factors in the main channel and the channel between the source and the eavesdropper.

¹Strictly speaking we must also assume a limit on the size of the eavesdropper's device, as this size-limit in effect places an upper limit of the number of (useful) antennas at the eavesdropper.

The work of R. Malaney was supported by the Australian Research Council Discovery Project (DP120102607).

C. Liu and R. Malaney are with the School of Electrical Engineering and Telecommunications, The University of New South Wales, Sydney, NSW 2052, Australia (email: chenxi.liu@student.unsw.edu.au; r.malaney@unsw.edu.au).

- Based on this new expression, we develop a much more efficient search algorithm for the determination of the optimal beamforming scheme that minimizes the secrecy outage probability when the CSI of the main channel and the eavesdropper's location are available at the source. We highlight that our new search algorithm invokes a one-dimensional search, as opposed to the multi-dimensional searches required previously, thereby greatly reducing the computational complexity (important for in-filed deployment).
- We derive an approximate expression of the secrecy outage probability of the system with the jammer for the special case where the Rician K -factor of the jammer-eavesdropper channel is 0, which provides a computationally efficient way to characterize the secrecy outage probability of the system with the jammer when the jammer-eavesdropper channel is in a pure Rayleigh fading environment.
- We examine the impact of location uncertainty on the secrecy outage probability, showing how secrecy can still exist when only a noisy estimate of the eavesdropper's location is available at the source.

The rest of the paper is organized as follows. Section II describes the system model considered in the paper. In Section III, we detail the proposed LBB scheme in Rician wiretap channels without the jammer. In Section IV, we examine the proposed LBB scheme in Rician wiretap channels with the jammer. Numerical results and related discussions are presented in Section V. Finally, Section VI draws conclusions.

Notations: Column vectors (matrices) are denoted by bold-face lower (upper) case letters. Transpose and conjugate transpose are denoted by $(\cdot)^T$ and $(\cdot)^H$, respectively. Complex Gaussian distribution is denoted by \mathcal{CN} . An imaginary number is denoted by j . A $1 \times m$ zero vector is denoted by $\mathbf{0}_{1 \times m}$. An $m \times m$ zero matrix and an $m \times m$ identity matrix are denoted by $\mathbf{0}_m$ and \mathbf{I}_m , respectively. Statistical expectation and Statistical variance are denoted by \mathbb{E} and Var , respectively. The diagonal elements of a matrix is denoted by $\text{diag}[\cdot]$. The trace of a matrix is denoted by $\text{Tr}\{\cdot\}$. The absolute value of a scalar is denoted by $|\cdot|$. The Frobenius norm of a vector or a matrix is denoted by $\|\cdot\|$.

II. SYSTEM MODEL

We consider a wiretap channel with Rician fading consisting of a source (Alice), a destination (Bob), a Jammer (J), and an eavesdropper (Eve), as shown in Fig. 1. In this channel, Alice communicates with Bob in the presence of Eve. Simultaneously, J transmits the jamming signals to degrade the quality of the received signals at Eve, while maintaining the quality of the received signals at Bob. Alice, J, and Eve are equipped with uniform linear arrays (ULA) with N_a , N_j and N_e antennas, respectively, while Bob is equipped with a single antenna. We adopt the polar coordinate system. As such, the locations of Alice, Bob, J, and Eve are denoted by $(0, 0)$, (d_{ab}, θ_{ab}) , (d_{aj}, θ_{aj}) and (d_{ae}, θ_{ae}) , respectively. We assume that all the channels are subject to quasi-static independent and identically distributed (i.i.d) Rician fading with different

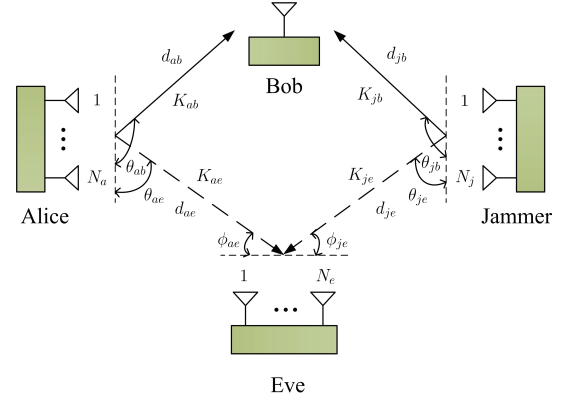


Fig. 1. Illustration of our wiretap channel with Rician fading. The Rician fading between all devices is assumed general, covering pure LOS through to pure Rayleigh fading. Real-world-channels lie somewhere in between these extremes. Note this figure serves to define the angles used in the main text (the angles ϕ_{ae} and ϕ_{je} will not enter the secrecy outcomes), and the distances between devices.

Rician K -factors. We assume that (via *a priori* measurement campaigns) the K -factors and path loss exponents of all relevant channels are known, and that the CSI of the main channel between Alice and Eve is known to Alice. We also assume that the CSI of the J-Bob channel is known to J. We further assume that the available information on Eve at Alice is her location. This last assumption is reasonable in a wide range of scenarios [15]. Examples of which include: when a system we wish to avoid communication with is a known fixed base station; the adversary has a device whose radio signals we can detect (and therefore triangulate on); and a military scenario where the enemy's location is determined through some visual surveillance. To make progress we will first assume Eve's location is known exactly, turning to noisy estimates later in the paper.

We denote \mathbf{h}_{ab} as the $1 \times N_a$ channel vector from Alice to Bob, which is given by

$$\mathbf{h}_{ab} = \sqrt{\frac{K_{ab}}{1 + K_{ab}}} \mathbf{h}_{ab}^o + \sqrt{\frac{1}{1 + K_{ab}}} \mathbf{h}_{ab}^r, \quad (1)$$

where K_{ab} denotes the Rician K -factor of the main channel, \mathbf{h}_{ab}^o denotes the LOS component of the main channel, and \mathbf{h}_{ab}^r denotes the scattered component of the main channel - the elements of which are assumed to be i.i.d complex Gaussian random variables with zero mean and unit variance, i.e., $\mathbf{h}_{ab}^r \sim \mathcal{CN}(\mathbf{0}_{1 \times N_a}, \mathbf{I}_{N_a})$. In (1), \mathbf{h}_{ab}^o is expressed as [17]

$$\mathbf{h}_{ab}^o = [1, \dots, \exp(j2\pi(N_a - 1)\delta_a \cos \theta_{ab})], \quad (2)$$

where δ_a denotes the constant spacing, in wavelengths, between adjacent antennas of the ULA at Alice. We also denote \mathbf{h}_{jb} as the $1 \times N_j$ channel vector from J to Bob as

$$\mathbf{h}_{jb} = \sqrt{\frac{K_{jb}}{1 + K_{jb}}} \mathbf{h}_{jb}^o + \sqrt{\frac{1}{1 + K_{jb}}} \mathbf{h}_{jb}^r, \quad (3)$$

where K_{jb} denotes the Rician K -factor of the J-Bob channel, \mathbf{h}_{jb}^o denotes the LOS component of the J-Bob channel, and \mathbf{h}_{jb}^r denotes the scattered component of the J-Bob channel - the

elements of which are assumed to be i.i.d complex Gaussian random variables with zero mean and unit variance, i.e., $\mathbf{h}_{jb}^r \sim \mathcal{CN}(\mathbf{0}_{1 \times N_j}, \mathbf{I}_{N_j})$. In (3), \mathbf{h}_{jb}^o is expressed as

$$\mathbf{h}_{jb}^o = [1, \dots, \exp(j2\pi(N_j - 1)\delta_j \cos \theta_{jb})], \quad (4)$$

where δ_j denotes the constant spacing, in wavelengths, between adjacent antennas of the ULA at J, and θ_{jb} denotes the angle from J to Bob.

We denote \mathbf{G}_{ae} as the $N_e \times N_a$ channel matrix from Alice to Eve, which is given by

$$\mathbf{G}_{ae} = \sqrt{\frac{K_{ae}}{1 + K_{ae}}} \mathbf{G}_{ae}^o + \sqrt{\frac{1}{1 + K_{ae}}} \mathbf{G}_{ae}^r, \quad (5)$$

where K_{ae} denotes the Rician K -factor of the Alice-Eve channel, \mathbf{G}_{ae}^o denotes the LOS component of the Alice-Eve channel, and \mathbf{G}_{ae}^r denotes the scattered component of the Alice-Eve channel - the elements of which are assumed to be i.i.d complex Gaussian random variables with zero mean and unit variance, i.e., $\mathbf{G}_{ae}^r \sim \mathcal{CN}(\mathbf{0}_{N_e \times N_a}, \mathbf{I}_{N_e})$. In (5), \mathbf{G}_{ae}^o is expressed as [18]

$$\mathbf{G}_{ae}^o = (\mathbf{r}_{ae}^o)^T \mathbf{g}_{ae}^o, \quad (6)$$

where \mathbf{r}_{ae}^o denotes the array responses of Alice's transmitted signals at Eve, which is given by

$$\mathbf{r}_{ae}^o = [1, \dots, \exp(-j2\pi(N_e - 1)\delta_e \cos \phi_{ae})], \quad (7)$$

where δ_e denotes the constant spacing, in wavelengths, between adjacent antennas of the ULA at Eve, and ϕ_{ae} denotes the angle of arrival from Eve to Alice (see Fig. 1), and \mathbf{g}_{ae}^o denotes the array response at Alice, which is given by

$$\mathbf{g}_{ae}^o = [1, \dots, \exp(j2\pi(N_a - 1)\delta_a \cos \theta_{ae})]. \quad (8)$$

We also denote \mathbf{G}_{je} as the $N_e \times N_j$ channel matrix from J to Eve as

$$\mathbf{G}_{je} = \sqrt{\frac{K_{je}}{1 + K_{je}}} \mathbf{G}_{je}^o + \sqrt{\frac{1}{1 + K_{je}}} \mathbf{G}_{je}^r, \quad (9)$$

where K_{je} denotes the Rician K -factor of the J-Eve channel, \mathbf{G}_{je}^o denotes the LOS component of the J-Eve channel, and \mathbf{G}_{je}^r denotes the scattered component of the J-Eve channel - the elements of which are assumed to be i.i.d complex Gaussian random variables with zero mean and unit variance, i.e., $\mathbf{G}_{je}^r \sim \mathcal{CN}(\mathbf{0}_{N_e \times N_j}, \mathbf{I}_{N_e})$. In (9), \mathbf{G}_{je}^o is expressed as

$$\mathbf{G}_{je}^o = (\mathbf{r}_{je}^o)^T \mathbf{g}_{je}^o, \quad (10)$$

where \mathbf{r}_{je}^o denotes the array responses of J's transmitted signals at Eve, which is given by

$$\mathbf{r}_{je}^o = [1, \dots, \exp(-j2\pi(N_e - 1)\delta_e \cos \phi_{je})], \quad (11)$$

where ϕ_{je} denotes the angle of arrival from Eve to J, and \mathbf{g}_{je}^o denotes the array response at J, which is given by

$$\mathbf{g}_{je}^o = [1, \dots, \exp(j2\pi(N_j - 1)\delta_j \cos \theta_{je})], \quad (12)$$

where θ_{je} denotes the angle from J to Eve.

We assume that J transmits the jamming signal to degrade the quality of the received signal at Eve, while maintaining

the quality of the received signal at Bob. As such, we design the jamming signal from J as

$$\mathbf{x}_{AN} = \mathbf{W}_{AN} \mathbf{t}_{AN}, \quad (13)$$

where \mathbf{W}_{AN} is an $N_j \times (N_j - 1)$ beamforming matrix used to transmit the jamming signal, and \mathbf{t}_{AN} is an $(N_j - 1) \times 1$ vector of the jamming signal. In designing \mathbf{x}_{AN} , we choose \mathbf{W}_{AN} as the orthonormal basis of the null space of \mathbf{h}_{jb} . We then choose \mathbf{t}_{AN} to satisfy $\mathbb{E}[\mathbf{t}_{AN} \mathbf{t}_{AN}^H] = \frac{1}{N_j - 1} \mathbf{I}_{N_j - 1}$. Such a design ensures that $\text{Tr}\{\mathbf{x}_{AN} \mathbf{x}_{AN}^H\} = 1$.

According to (1)-(13), we express the received signal at Bob as

$$y_b = \sqrt{P_a d_{ab}^{-\eta_{ab}}} \mathbf{h}_{ab} \mathbf{x}_a + n_b, \quad (14)$$

where P_a denotes the transmit power at Alice, η_{ab} denotes the path loss exponent of the main channel (as in [15] all path loss exponents will be a function of the sender-receiver channel, i.e. device locations), and n_b denotes the thermal noise at Bob - which is assumed to be a complex Gaussian random variable with zero mean and variance σ_b^2 , i.e., $n_b \sim \mathcal{CN}(0, \sigma_b^2)$. In (14), \mathbf{x}_a is expressed as

$$\mathbf{x}_a = \mathbf{w} t_a, \quad (15)$$

where \mathbf{w} denotes the $N_a \times 1$ beamforming vector², and t_a is a scalar, which denotes the information signal transmitted by Alice. We assume that $\|\mathbf{w}\|^2 = 1$ and $\mathbb{E}[|t_a|^2] = 1$. We then express the received signal at Eve as

$$\mathbf{y}_e = \sqrt{P_a d_{ae}^{-\eta_{ae}}} \mathbf{G}_{ae} \mathbf{x}_a + \sqrt{P_j d_{je}^{-\eta_{je}}} \mathbf{G}_{je} \mathbf{x}_{AN} + \mathbf{n}_e, \quad (16)$$

where P_j denotes the transmit power at J, d_{je} denotes the distance between J and Eve, η_{ae} and η_{je} denote the path loss exponents in the Alice-Eve channel and J-Eve channel, respectively, and \mathbf{n}_e denotes the thermal noise vector at Eve - the elements of which are assumed to be i.i.d complex Gaussian random variables with zero mean and variance σ_e^2 , i.e., $\mathbf{n}_e \sim (\mathbf{0}_{N_e \times 1}, \mathbf{I}_{N_e})$.

As such, we express the received SNR at Bob as

$$\gamma_b = \tilde{\gamma}_{ab} |\mathbf{h}_{ab} \mathbf{w}|^2, \quad (17)$$

where $\tilde{\gamma}_{ab} = P_a d_{ab}^{-\eta_{ab}} / \sigma_b^2$.

In order to maximize the probability of successful eavesdropping, we assume that Eve applies the minimum mean square error (MMSE) combining to process her received signal. As per the rules of MMSE combining [21], we express the instantaneous SNR at Eve as

$$\gamma_e = \tilde{\gamma}_{ae} \mathbf{w}^H \mathbf{G}_{ae}^H \mathbf{M}^{-1} \mathbf{G}_{ae} \mathbf{w}, \quad (18)$$

where $\tilde{\gamma}_{ae} = P_a d_{ae}^{-\eta_{ae}} / \sigma_e^2$ and

$$\mathbf{M} = \frac{\tilde{\gamma}_{je}}{N_j - 1} \mathbf{G}_{je} \mathbf{W}_{AN} \mathbf{W}_{AN}^H \mathbf{G}_{je}^H + \mathbf{I}_{N_e} \quad (19)$$

with $\tilde{\gamma}_{je} = P_j d_{je}^{-\eta_{je}} / \sigma_e^2$.

²We correct a typographical error in [19] here by setting \mathbf{w} as a row vector.

Based on (17) and (18), the achievable secrecy rate in the wiretap channel is expressed as [20]

$$C_s = \begin{cases} C_b - C_e, & \gamma_b > \gamma_e \\ 0, & \gamma_e \leq \gamma_e, \end{cases} \quad (20)$$

where $C_b = \log_2(1 + \gamma_b)$ is the capacity of the main channel, and $C_e = \log_2(1 + \gamma_e)$ is the capacity of the Alice-Eve channel. In this wiretap channel, if $C_s \geq R_s$, where R_s denotes a given secrecy transmission rate, the perfect secrecy is guaranteed. If $C_s < R_s$, information on the transmitted signal is leaked to Eve, and the secrecy is compromised. In order to evaluate the secrecy performance of the wiretap channel in detail, we adopt the secrecy outage probability as the performance metric - defined as the probability that the achievable secrecy rate is less than a given secrecy transmission rate conditioned on γ_b . Mathematically, this is formulated as

$$P_{\text{out}}(R_s) = \Pr(C_s < R_s | \gamma_b). \quad (21)$$

Our goal is to find the optimal beamforming vector that minimizes the secrecy outage probability. That is, we wish to find

$$\mathbf{w}^* = \underset{\mathbf{w}, \|\mathbf{w}\|^2=1}{\operatorname{argmin}} P_{\text{out}}(R_s). \quad (22)$$

III. LOCATION-BASED BEAMFORMING WITHOUT JAMMER

In this section we assume that J is not transmitting (i.e., $P_j = 0$), describing in detail how the optimal beamforming scheme (that minimizes the secrecy outage probability) is obtained through the use of Bob's CSI and Eve's location. We also derive an easy-to-compute expression for the secrecy outage probability when the proposed LBB scheme is applied.

We first re-express \mathbf{y}_e in (16) when J is not transmitting as

$$\mathbf{y}_e = \sqrt{P_a d_{ae}^{-\eta_{ae}}} \mathbf{G}_{ae} \mathbf{x}_a + \mathbf{n}_e. \quad (23)$$

We then re-express γ_e in (18) when J is not transmitting as

$$\gamma_e = \tilde{\gamma}_{ae} \|\mathbf{G}_{ae} \mathbf{w}\|^2. \quad (24)$$

In order to solve (22), we present the following proposition.

Proposition 1: Given $\tau \in [0, 1]$, the optimal beamforming vector \mathbf{w}^* that minimizes the secrecy outage probability is a member of the following family of beamformer solutions,

$$\mathbf{w}(\tau) = \sqrt{\tau} \mathbf{w}_1 + \sqrt{1 - \tau} \mathbf{w}_2. \quad (25)$$

Here, $\mathbf{w}_1 = \frac{\Psi_{\mathbf{G}_{ae}^o}^\perp \mathbf{h}_{ab}^H}{\|\Psi_{\mathbf{G}_{ae}^o}^\perp \mathbf{h}_{ab}^H\|}$, where $\Psi_{\mathbf{G}_{ae}^o}^\perp = \mathbf{I}_{N_a} - (\mathbf{G}_{ae}^o)^H (\mathbf{G}_{ae}^o (\mathbf{G}_{ae}^o)^H)^{-1} \mathbf{G}_{ae}^o$; and $\mathbf{w}_2 = \frac{\Psi_{\mathbf{G}_{ae}^o} \mathbf{h}_{ab}^H}{\|\Psi_{\mathbf{G}_{ae}^o} \mathbf{h}_{ab}^H\|}$, where $\Psi_{\mathbf{G}_{ae}^o} = (\mathbf{G}_{ae}^o)^H (\mathbf{G}_{ae}^o (\mathbf{G}_{ae}^o)^H)^{-1} \mathbf{G}_{ae}^o$.

Proof: Suppose that $\{\mathbf{w}_1, \mathbf{w}_2, \mathbf{w}_3, \dots, \mathbf{w}_{N_a}\}$ denotes an orthonormal basis in the complex space \mathbb{C}^{N_a} . As such, any beamforming vector at Alice can be expressed as [22]

$$\mathbf{w} = \lambda_1 \mathbf{w}_1 + \lambda_2 \mathbf{w}_2 + \sum_{l=3}^{N_a} \lambda_l \mathbf{w}_l, \quad (26)$$

where $\lambda = [\lambda_1, \lambda_2, \dots, \lambda_{N_a}]$ are complex and $\|\lambda\|^2 = 1$. We first note that the achievable secrecy rate C_s is a function of \mathbf{w} .

We then note that beamforming into \mathbf{w}_l has no impact on the capacity of the main channel C_b . This is due to the fact that \mathbf{w}_l are orthogonal to the plane spanned by $\{\mathbf{w}_1, \mathbf{w}_2\}$ and the main channel \mathbf{h}_{ab} lies in this plane. We also find that beamforming into \mathbf{w}_l , on the other hand, may increase the capacity of Alice-Eve channel C_e unless the Alice-Eve channel \mathbf{G}_{ae} also lies in the plane spanned by $\{\mathbf{w}_1, \mathbf{w}_2\}$.

Based on the above analysis, we see that beamforming into \mathbf{w}_l decreases C_s or has no impact on C_s . As such, we confirm that the optimal beamforming vector has the following structure, given by

$$\mathbf{w}(\tau) = \underbrace{\sqrt{\tau} \exp(j\theta_1)}_{\lambda_1} \mathbf{w}_1 + \underbrace{\sqrt{1 - \tau} \exp(j\theta_2)}_{\lambda_2} \mathbf{w}_2. \quad (27)$$

We note that θ_1 and θ_2 in (27) are general phases having no impact on C_s , thus without loss of generality we can set $\theta_1 = \theta_2 = 0$. Substituting $\theta_1 = \theta_2 = 0$ into (27) we obtain the desired result in (25), which completes the proof. ■

With the aid of *Proposition 1*, we note that the optimal beamforming vector \mathbf{w}^* that solves (22) can be obtained by finding the optimal τ^* that minimizes the secrecy outage probability. As such, we re-express (22) as

$$\tau^* = \underset{0 \leq \tau \leq 1}{\operatorname{argmin}} P_{\text{out}}(R_s). \quad (28)$$

We highlight that *Proposition 1* provides a far more efficient way of obtaining the optimal beamforming vector \mathbf{w}^* that solves (22) compared to an exhaustive search. This is due to the fact that an exhaustive search is performed in the complex space \mathbb{C}^{N_a} . Consequently, the computational complexity of the exhaustive search grows exponentially as N_a increases. This is to be compared with our method in *Proposition 1* which involves a one-dimensional search of τ^* only, regardless of the value of N_a .

We now present the expression of the secrecy outage probability when $\mathbf{w}(\tau)$ is adopted as the beamforming vector in the following theorem.

Theorem 1: The secrecy outage probability when $\mathbf{w}(\tau) = \sqrt{\tau} \mathbf{w}_1 + \sqrt{1 - \tau} \mathbf{w}_2$ is adopted as the beamforming vector is given by

$$P_{\text{out}}(R_s) = 1 - \frac{\gamma\left(N_e \hat{m}_{ae}, \frac{2^{-R_s}(1+\gamma_b)-1}{\hat{m}_{ae}^{-1} \tilde{\gamma}_e}\right)}{\Gamma(N_e \hat{m}_{ae})}, \quad (29)$$

where $\gamma(\cdot, \cdot)$ is the lower incomplete gamma function, defined as [23, Eq. (8.350)],

$$\gamma(\mu, \nu) = \int_0^\nu \exp(-t) t^{\mu-1} dt, \quad (30)$$

$$\hat{m}_{ae} = \frac{(\hat{K}_{ae} + 1)^2}{2\hat{K}_{ae} + 1}, \quad (31)$$

where $\hat{K}_{ae} = |\mathbf{g}_{ae}^o \mathbf{w}(\tau)|^2 K_{ae}$,

$$\tilde{\gamma}_e = \mathbb{E}[\gamma_e] = \frac{(K_{ae} |\mathbf{g}_{ae}^o \mathbf{w}(\tau)|^2 + 1) \tilde{\gamma}_{ae}}{1 + K_{ae}}, \quad (32)$$

and $\Gamma(\cdot)$ is the Gamma function, defined as [23, Eq. (8.310)],

$$\Gamma(z) = \int_0^\infty \exp(-t) t^{z-1} dt. \quad (33)$$

Proof: We focus on the probability density function (PDF) of γ_e when $\mathbf{w}(\tau)$ is adopted as the beamforming vector, which is expressed as [15]

$$f_{\gamma_e}(x) = \left(\frac{\hat{m}_{ae}}{\bar{\gamma}_e} \right)^{N_e \hat{m}_{ae}} \frac{x^{N_e \hat{m}_{ae} - 1}}{\Gamma(N_e \hat{m}_{ae})} \exp\left(-\frac{\hat{m}_{ae} x}{\bar{\gamma}_e}\right). \quad (34)$$

The cumulative distribution function (CDF) of γ_e is then obtained as

$$F_{\gamma_e}(x) = \frac{\gamma\left(N_e \hat{m}_{ae}, \frac{\hat{m}_{ae} x}{\bar{\gamma}_e}\right)}{\Gamma(N_e \hat{m}_{ae})}. \quad (35)$$

Based on (23) and (24), we re-express $P_{\text{out}}(R_s)$ in (21) when J is not transmitting as

$$\begin{aligned} P_{\text{out}}(R_s) &= \Pr(C_b - C_e < R_s | \gamma_b) \\ &= \Pr(C_e > C_b - R_s | \gamma_b) \\ &= \Pr(\gamma_e > 2^{-R_s} (1 + \gamma_b) - 1) \\ &= 1 - F_{\gamma_e}(2^{-R_s} (1 + \gamma_b) - 1). \end{aligned} \quad (36)$$

Substituting (35) into (36), we obtain the desired result in *Theorem 1*. The proof is completed. ■

Note, in *Theorem 1* Eve's location is explicitly expressed in the expressions for \hat{m}_{ae} , \hat{K}_{ae} , and $\bar{\gamma}_e$. Note also, that our derived expression is valid for arbitrary values of average SNRs and Rician K -factors in the main channel and the Alice-Eve channel. In the following, we detail how the optimal τ^* that minimizes $P_{\text{out}}(R_s)$ can be obtained per block by applying **Algorithm 1**.

Algorithm 1 Algorithm to determine τ^* per block when J is not transmitting

Input: \mathbf{h}_{ab}

Output: τ^* .

- 1: Calculate \mathbf{w}_1 and \mathbf{w}_2 .
 - 2: **for** every $\tau \in [0, 1]$ with step size δ_t **do**
 - 3: Calculate $\mathbf{w}(\tau)$ using (25).
 - 4: Calculate $P_{\text{out}}(R_s)$ using (29).
 - 5: **end for**
 - 6: Choose τ^* as the value of τ that achieves the minimum $P_{\text{out}}(R_s)$.
-

We now evaluate the computational demands of **Algorithm 1**. For a given N_a , N_e , and δ_t , **Algorithm 1** requires $2\delta_t^{-1}$ gamma function calculations. We note that the complexity for the gamma function calculation is $O(n^{5/2}(\log n)^2)$ [24], where n denotes the number of digits used. For anticipated values of N_a , N_e , $\delta_t = 10^{-2}$, and assuming 64-bit processing, the number of floating-point operations for **Algorithm 1** is of order 10^6 (note, $\delta_t = 10^{-2}$ leads to a negligible error of 1 part in 10^4 compared to the true minimum secrecy outage probability). Assuming 4 floating-point operations per cycle, 10^6 operations can be completed on a single-core 64-bit 2.5 GHz microprocessor within 1 ms. As such, **Algorithm 1** can

be performed in real-time with negligible latency impact³. On the other hand, an exhaustive search of the optimal beamforming vector \mathbf{w}^* that minimizes $P_{\text{out}}(R_s)$ requires $2(\delta_t^{-1})^{2N_a}$ gamma function calculations. We note that $2(\delta_t^{-1})^{2N_a}$ gamma function calculations require of order 10^{12} floating-point operations for $N_a = 2$, and $\delta_t = 10^{-2}$. Moreover, the number of floating-point operations for an exhaustive search grows exponentially with N_a . As such, an exhaustive search is simply not practical in real-world deployments.

We point out that ϕ_{ae} disappears in the expression for the secrecy outage probability in *Theorem 1*. As an aside, it is perhaps interesting to show why this is so. To this end, we re-express γ_e in (24) as

$$\gamma_e = \tilde{\gamma}_{ae} \sum_{i=1}^{N_e} |\mathbf{g}_{ae,i} \mathbf{w}(\tau)|^2, \quad (37)$$

where $\mathbf{g}_{ae,i}$ is the $1 \times N_a$ channel vector between Alice and i -th Eve's antenna, given by

$$\mathbf{g}_{ae,i} = \sqrt{\frac{K_{ae}}{1 + K_{ae}}} r_{ae,i}^o \mathbf{g}_{ae}^o + \sqrt{\frac{1}{1 + K_{ae}}} \mathbf{g}_{ae,i}^r, \quad (38)$$

where $r_{ae,i}^o$ is the i -th element of \mathbf{r}_{ae}^o , given by $r_{ae,i}^o = \exp(-j2\pi(i-1)\delta_e \cos \phi_{ae})$ and $\mathbf{g}_{ae,i}^r$ is the i -th row of \mathbf{G}_{ae}^r . Based on (38), we express $\mathbf{g}_{ae,i} \mathbf{w}(\tau)$ as

$$\begin{aligned} \mathbf{g}_{ae,i} \mathbf{w}(\tau) &= \sqrt{\frac{K_{ae}}{1 + K_{ae}}} r_{ae,i}^o \mathbf{g}_{ae}^o \mathbf{w}(\tau) \\ &\quad + \sqrt{\frac{1}{1 + K_{ae}}} \mathbf{g}_{ae,i}^r \mathbf{w}(\tau). \end{aligned} \quad (39)$$

We note that $|r_{ae,i}^o \mathbf{g}_{ae}^o \mathbf{w}(\tau)|^2 = |\mathbf{g}_{ae}^o \mathbf{w}(\tau)|^2$ for any $r_{ae,i}^o$. As such, we confirm that the value of ϕ_{ae} has no impact on the secrecy outage probability. This reveals that our analysis reported here is also applicable for antenna arrays other than ULA at Eve.

IV. LOCATION-BASED BEAMFORMING WITH JAMMER

In this section we examine the case when J is transmitting (i.e., $P_j > 0$). We shall see of course that a jammer assists the performance. We will also see that, in principal, a modified (more complex) **Algorithm 1** can be used to determine the optimal beamformer in the presence of the jammer. However, we will also see that the previous beamforming solution derived directly from **Algorithm 1**, when used in the presence of a jammer, leads to a performance that is very close to optimal when the number of antenna at Alice is greater than two. This means that in practice the beamforming solution derived from **Algorithm 1** will actually suffice in most circumstances.

To make progress, we present the following proposition.

Proposition 2: Given $\tau \in [0, 1]$, the optimal beamforming vector \mathbf{w}^* that minimizes the secrecy outage probability of

³The computation time of **Algorithm 1** on MATLAB is less than 0.25 s on a quad-core 64-bit 3.3 GHz Intel i5-2500 microprocessor. Based on the conversion factor from MATLAB to embedded C++ firmware, we estimate the per block latency to be less than 0.5 ms [25], while the coherence time of the channel is hundreds of milliseconds for stationary nodes [26].

Rician wiretap channels with a jammer is also a member of the following family of beamformer solutions,

$$\mathbf{w}(\tau) = \sqrt{\tau}\mathbf{w}_1 + \sqrt{1-\tau}\mathbf{w}_2. \quad (40)$$

Proof: Let $\mathbf{R} = \frac{\tilde{\gamma}_{je}}{N_j-1}\mathbf{G}_{je}\mathbf{W}_{AN}\mathbf{W}_{AN}^H\mathbf{G}_{je}^H$, the eigenvalue decomposition of \mathbf{R} is given by $\mathbf{R} = \mathbf{U}^H\mathbf{\Lambda}\mathbf{U}$, where \mathbf{U} is an $N_e \times N_e$ unitary matrix, and $\mathbf{\Lambda} = \text{diag}[\Lambda_1, \dots, \Lambda_{N_e}]$, and where $\Lambda_1, \dots, \Lambda_{N_e}$ are eigenvalues of \mathbf{R} . Based on \mathbf{R} and $\mathbf{\Lambda}$, we re-express the instantaneous SNR at Eve in (18) as

$$\begin{aligned} \gamma_e &= \tilde{\gamma}_{ae}\mathbf{w}^H\mathbf{G}_{ae}^H\mathbf{U}^H(\mathbf{\Lambda} + \mathbf{I}_{N_e})^{-1}\mathbf{U}\mathbf{G}_{ae}\mathbf{w} \\ &= \tilde{\gamma}_{ae}[\mu_1^H, \dots, \mu_{N_e}^H] \begin{bmatrix} \frac{1}{\Lambda_1+1}, & \dots, & 0 \\ \vdots & \ddots & \vdots \\ 0, & \dots, & \frac{1}{\Lambda_{N_e}+1} \end{bmatrix} \begin{bmatrix} \mu_1 \\ \vdots \\ \mu_{N_e} \end{bmatrix} \\ &= \sum_{i=1}^{N_e} \frac{|\mu_i|^2}{\Lambda_i + 1}, \end{aligned} \quad (41)$$

where u_i denotes the i -th element of $\mathbf{U}\mathbf{G}_{ae}\mathbf{w}$. Suppose ν_i is the i -th element of $\mathbf{G}_{ae}\mathbf{w}$, we express the instantaneous SNR at Eve when J is not transmitting as

$$\begin{aligned} \gamma_e &= \tilde{\gamma}_{ae}\mathbf{w}^H\mathbf{G}_{ae}^H\mathbf{G}_{ae}\mathbf{w} \\ &= \tilde{\gamma}_{ae}[\nu_1^H, \dots, \nu_{N_e}^H] \begin{bmatrix} \nu_1 \\ \vdots \\ \nu_{N_e} \end{bmatrix} \\ &= \tilde{\gamma}_{ae} \sum_{i=1}^{N_e} |\nu_i|^2. \end{aligned} \quad (42)$$

We note that ν_i and μ_i have the same PDF due to the fact that \mathbf{U} is a unitary matrix. We re-express $P_{\text{out}}(R_s)$ in (21) as

$$\begin{aligned} P_{\text{out}}(R_s) &= \Pr(C_b - C_e < R_s | \gamma_b) \\ &= \Pr(C_e > C_b - R_s | \gamma_b) \\ &= \Pr(\gamma_e > 2^{-R_s}(1 + \gamma_b) - 1) \\ &= \Pr\left(\tilde{\gamma}_{ae} \sum_{i=1}^{N_e} \frac{|\mu_i|^2}{\Lambda_i + 1} > 2^{-R_s}(1 + \gamma_b) - 1\right) \\ &= \Pr\left(\tilde{\gamma}_{ae} \sum_{i=1}^{N_e} |\mu_i|^2 > \frac{1}{k}(2^{-R_s}(1 + \gamma_b) - 1)\right), \end{aligned} \quad (43)$$

where $k = \frac{\sum_{i=1}^{N_e} \frac{|\mu_i|^2}{\Lambda_i + 1}}{\sum_{i=1}^{N_e} |\mu_i|^2}$. We then re-express $P_{\text{out}}(R_s)$ in (21) when J is not transmitting as

$$P_{\text{out}}(R_s) = \Pr\left(\tilde{\gamma}_{ae} \sum_{i=1}^{N_e} |\nu_i|^2 > 2^{-R_s}(1 + \gamma_b) - 1\right). \quad (44)$$

Since ν_i and μ_i have the same PDF, we re-write (43) as

$$\begin{aligned} P_{\text{out}}(R_s) &= \Pr\left(\tilde{\gamma}_{ae} \sum_{i=1}^{N_e} |\mu_i|^2 > \frac{1}{k}(2^{-R_s}(1 + \gamma_b) - 1)\right) \\ &= \Pr\left(\tilde{\gamma}_{ae} \sum_{i=1}^{N_e} |\nu_i|^2 > \frac{1}{k}(2^{-R_s}(1 + \gamma_b) - 1)\right). \end{aligned} \quad (45)$$

Observing (44) and (45), we find that the only difference between $P_{\text{out}}(R_s)$ when J is not transmitting and $P_{\text{out}}(R_s)$

when J is transmitting is the factor k^{-1} . Therefore, our analysis in *Proposition 1*, which is suitable for Rician wiretap channels without the jammer, still holds for channels with the jammer. According to *Proposition 1*, the optimal beamforming vector that minimizes $P_{\text{out}}(R_s)$ when J is not transmitting is a member of the family of beamformer solutions, given by $\mathbf{w}(\tau) = \sqrt{\tau}\mathbf{w}_1 + \sqrt{1-\tau}\mathbf{w}_2$. As such, we obtain that the optimal beamforming vector that minimizes $P_{\text{out}}(R_s)$ when J is transmitting is also a member of such a family of beamformer solutions. We note that the optimal value of τ that minimizes $P_{\text{out}}(R_s)$ when J is transmitting is different from the optimal τ^* that minimizes $P_{\text{out}}(R_s)$ when J is not transmitting due to the factor k^{-1} . The proof is completed. ■

According to *Proposition 2*, we note that the optimal \mathbf{w}^* at Alice that minimizes $P_{\text{out}}(R_s)$ can be obtained by determining the optimal τ_j^* that minimizes $P_{\text{out}}(R_s)$ when J is transmitting. As such, we re-express (22) as

$$\tau_j^* = \underset{0 \leq \tau \leq 1}{\text{argmin}} P_{\text{out}}(R_s). \quad (46)$$

We note that the analytical form of $P_{\text{out}}(R_s)$ for general K_{je} is mathematically intractable. As such, in order to obtain the optimal τ_j^* that minimizes $P_{\text{out}}(R_s)$, we apply a modified **Algorithm 1**, in which we numerically calculate $P_{\text{out}}(R_s)$. Specifically, we first generate N realizations of \mathbf{G}_{ae}^r and \mathbf{G}_{je}^r , we then calculate C_s using (20) for every \mathbf{G}_{ae}^r and \mathbf{G}_{je}^r . Finally, we calculate $P_{\text{out}}(R_s)$ using (21). For the same level of performance we find the modified algorithm costs approximately 10 times more computational time relative to **Algorithm 1** - and therefore is still viable in real-world deployments. However, as we discuss later, we shall see that in practice the solution provided directly by **Algorithm 1** will actually suffice in most circumstances - even when the jammer is present.

Moreover, we find that an approximate expression of $P_{\text{out}}(R_s)$ for the special case where $K_{je} = 0$ is obtainable. We note that such a special case is practical in scenarios where the J-Eve channel is completely blocked (e.g. Eve is in hiding) by buildings. In order to examine the approximate expression of $P_{\text{out}}(R_s)$ for the special case where $K_{je} = 0$, we first introduce several new notations as follows:

$$\varphi_l = \frac{1}{(1 + K_{ae})^l} \sum_{m=0}^l \binom{l}{m} \frac{(K_{ae}|\mathbf{G}_{ae}^o\mathbf{w}(\tau)|^2)^m}{(N_e)_m}, l \in \{1, 2\} \quad (47)$$

with $(N_e)_m = \frac{\Gamma(N_e+m)}{\Gamma(N_e)}$, and

$$\begin{aligned} \vartheta_l &= \frac{l \exp\left(\frac{1}{\kappa}\right)}{\kappa^{N_j-1}} \sum_{p=0}^{N_e-1} \rho_p \sum_{t=0}^{l-1+p} \binom{l-1+p}{t} \left(-\frac{1}{\kappa}\right)^{l-1+p-t} \\ &\quad \times \Gamma\left(t - N_j + 2, \frac{1}{\kappa}\right), \end{aligned} \quad (48)$$

respectively. In (48), $\kappa = \frac{\tilde{\gamma}_{je}}{N_j-1}$,

$$\rho_p = \kappa^p \sum_{q=\max(0, p-N_j+1)}^p \binom{N_j-1}{p-q} \frac{1}{q! \kappa^q}, \quad (49)$$

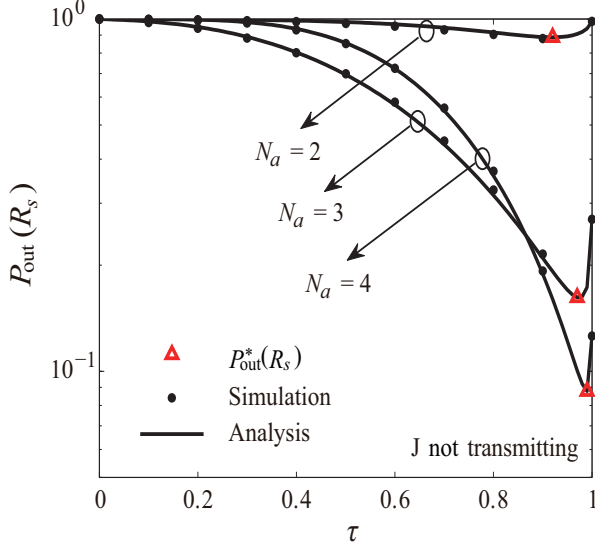


Fig. 2. $P_{\text{out}}(R_s)$ versus τ for different values of N_a with $N_e = 2$, $K_{ab} = 10$ dB, $K_{ae} = 5$ dB, $\tilde{\gamma}_{ab} = \tilde{\gamma}_{ae} = 10$ dB, $\theta_{ab} = \pi/3$, $\theta_{ae} = \pi/4$, and $R_s = 1$ bits/s/Hz. J is not transmitting here.

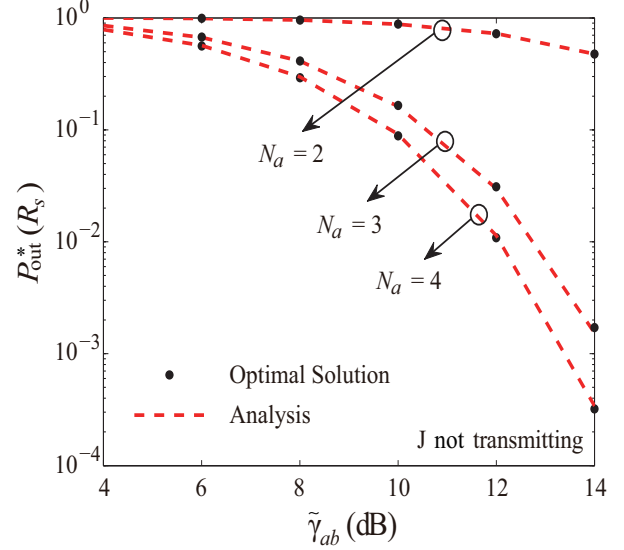


Fig. 3. $P_{\text{out}}^*(R_s)$ versus $\tilde{\gamma}_{ab}$ for different values of N_a with $N_e = 2$, $K_{ab} = 10$ dB, $K_{ae} = 5$ dB, $\tilde{\gamma}_{ae} = 10$ dB, $\theta_{ab} = \pi/3$, $\theta_{ae} = \pi/4$, and $R_s = 1$ bits/s/Hz. J is not transmitting here.

and $\Gamma(\cdot, \cdot)$ is the upper incomplete Gamma function, defined as [23, Eq. (8.350)]

$$\Gamma(\mu, \nu) = \int_{\nu}^{\infty} \exp(-t) t^{\mu-1} dt. \quad (50)$$

Theorem 2: When $K_{je} = 0$, the approximate secrecy outage probability of Rician wiretap channels with a jammer is

$$P_{\text{out}}(R_s) = 1 - \frac{\gamma\left(\alpha, \frac{2^{-R_s}(1+\gamma_b)-1}{\beta}\right)}{\Gamma(\alpha)}, \quad (51)$$

where

$$\alpha = \frac{\varphi_1^2 \vartheta_1^2}{\varphi_2 \vartheta_2 - \varphi_1^2 \vartheta_1^2}, \quad (52)$$

and

$$\beta = \tilde{\gamma}_{ae} \frac{(\varphi_2 \vartheta_2 - \varphi_1^2 \vartheta_1^2)}{\varphi_1 \vartheta_1}. \quad (53)$$

Proof: See Appendix A. ■

We highlight that the approximate expression of the secrecy outage probability in (51) is valid for arbitrary values of average SNRs and Rician K -factors in the main channel and the Alice-Eve channel.

V. NUMERICAL RESULTS

In this section, we present numerical results to validate our analysis. Specifically, we first demonstrate the effectiveness of the proposed LBB scheme in Rician wiretap channels where only Alice, Bob, and Eve are involved. We then demonstrate the effectiveness of the scheme when J is transmitting. Finally, we examine the impact of Eve's location uncertainty on secrecy performance of the scheme. Throughout this section, we assume that all the channels have the same path loss exponent, i.e., $\eta_{ab} = \eta_{ae} = \eta_{je} = 4$.

We first examine the effectiveness of the scheme when J is not transmitting in Figs. 2–3. In Fig. 2, we plot $P_{\text{out}}(R_s)$ versus τ for different values of N_a with $N_e = 2$, $K_{ab} = 10$ dB, $K_{ae} = 5$ dB, $\tilde{\gamma}_{ab} = \tilde{\gamma}_{ae} = 10$ dB, $\theta_{ab} = \pi/3$, $\theta_{ae} = \pi/4$, and $R_s = 1$ bits/s/Hz. We first observe that the analytical curves, generated from *Proposition 1* and *Theorem 1*, precisely match the simulation points marked by black dots, thereby demonstrating the correctness of our analysis for $P_{\text{out}}(R_s)$ in *Proposition 1* and *Theorem 1*. Second, we see that there exists a unique τ^* that minimizes $P_{\text{out}}(R_s)$ for each N_a . Third, we see that the minimum $P_{\text{out}}(R_s)$, denoted by $P_{\text{out}}^*(R_s)$, decreases significantly as N_a increases. Furthermore, we observe that the optimal τ^* that achieves $P_{\text{out}}^*(R_s)$ approaches 1 as N_a increases. This reveals that the optimal beamforming vector \mathbf{w}^* that minimizes $P_{\text{out}}(R_s)$ approaches \mathbf{w}_1 as N_a increases.

In Fig. 3, we plot $P_{\text{out}}^*(R_s)$ versus $\tilde{\gamma}_{ab}$ for different values of N_a . In this figure, we have adopted the same system configurations as those in Fig. 2. The analytical curves, represented by red dashed lines, are generated from *Proposition 1* and *Theorem 1* with the optimal τ^* which minimizes $P_{\text{out}}(R_s)$ being selected for different values of N_a . The optimal beamformer solutions, represented by ‘•’ symbols, are obtained from minimizing $P_{\text{out}}(R_s)$ via an exhaustive search (i.e., a full multi-dimensional search) for different values of N_a . We first see that the minimum secrecy outage probability $P_{\text{out}}^*(R_s)$ achieved by our scheme is almost the same as the optimal beamformer solution found via exhaustive search. This shows the optimality of our scheme. Second, we see that $P_{\text{out}}^*(R_s)$ decreases significantly as N_a increases. This reveals that adding extra transmit antennas at Alice improves the secrecy of the adopted system. We further see that $P_{\text{out}}^*(R_s)$ monotonically decreases as $\tilde{\gamma}_{ab}$ increase. This reveals that the secrecy outage probability reduces when Alice uses a higher power to transmit.

We then examine the effectiveness of the scheme when J

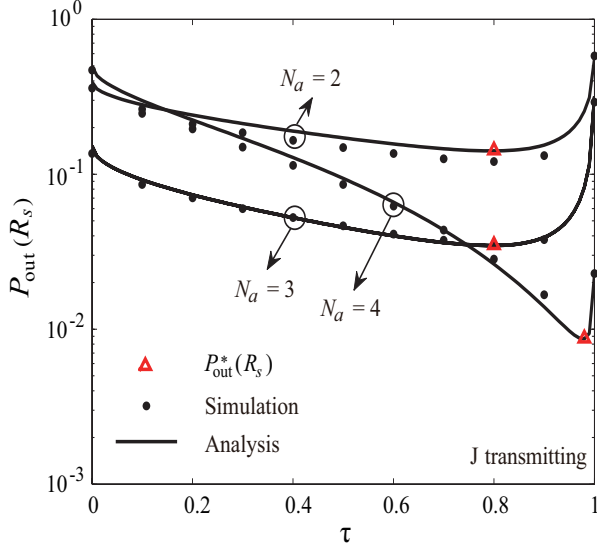


Fig. 4. $P_{\text{out}}(R_s)$ versus τ for different values of N_a with $N_e = 2$, $N_j = 4$, $K_{ab} = 10$ dB, $K_{ae} = 5$ dB, $K_{je} = 0$, $\tilde{\gamma}_{ab} = \tilde{\gamma}_{ae} = \tilde{\gamma}_{je} = 10$ dB, $\theta_{ab} = \pi/3$, $\theta_{ae} = \pi/4$, and $R_s = 1$ bits/s/Hz. J is transmitting here.

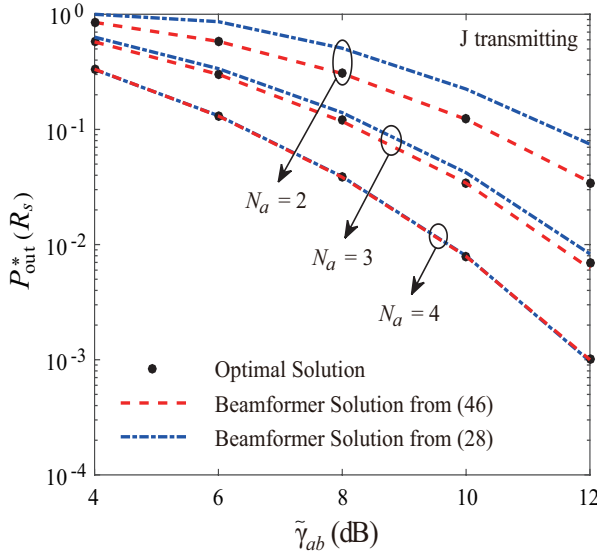


Fig. 5. $P_{\text{out}}^*(R_s)$ versus $\tilde{\gamma}_{ab}$ for different values of N_a with $N_e = 2$, $N_j = 4$, $K_{ab} = 10$ dB, $K_{ae} = 5$ dB, $K_{je} = 0$, $\tilde{\gamma}_{ae} = \tilde{\gamma}_{je} = 10$ dB, $\theta_{ab} = \pi/3$, $\theta_{ae} = \pi/4$, and $R_s = 1$ bits/s/Hz. J is transmitting here.

is transmitting in the following Figs. 4–5. To provide focus, we consider the special case of $K_{je} = 0$. In Fig. 4, we plot $P_{\text{out}}(R_s)$ versus τ for different values of N_a . We first see that the analytical curves, generated from *Proposition 2* and *Theorem 2*, match the simulation points, which validate our analysis in *Proposition 2* and *Theorem 2*. We then see that there exists a unique τ_j^* that minimizes $P_{\text{out}}(R_s)$ for each N_a . We also see that the optimal τ_j^* that minimizes $P_{\text{out}}(R_s)$ decreases for each N_a , compared to the optimal τ^* that minimizes $P_{\text{out}}(R_s)$ in Fig. 2. This is due to the fact that the jamming signals degrade the quality of the received signals at Eve.

In Fig. 5, we plot $P_{\text{out}}^*(R_s)$ versus $\tilde{\gamma}_{ab}$ for different values of

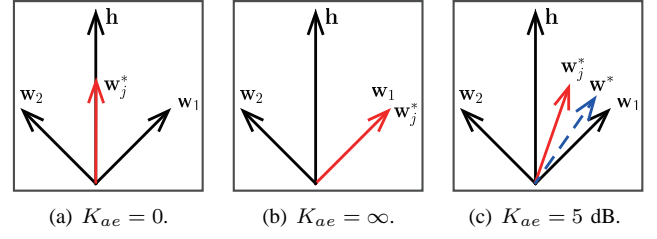


Fig. 6. Illustration of the optimal beamformer solutions for Rician wiretap channels with $N_a = 2$, $N_e = 2$, $K_{ab} = 10$ dB, $K_{je} = 0$, $\tilde{\gamma}_{ab} = \tilde{\gamma}_{ae} = \tilde{\gamma}_{je} = 10$ dB. \mathbf{w}^* and \mathbf{w}_j^* denote the optimal beamformer solution when J is not transmitting and the optimal beamformer solution when J is transmitting, respectively. \mathbf{w}^* and \mathbf{w}_j^* are represented by blue dashed line and red solid line, respectively.

N_a . In this figure, we compare the secrecy performance of the beamformer solution obtained from *Proposition 1* and *Theorem 1* and the beamformer solution obtained from *Proposition 2* and *Theorem 2* to the secrecy performance of the optimal beamformer solution. The beamformer solution obtained from *Proposition 1* and *Theorem 1* and the beamformer solution obtained from *Proposition 2* and *Theorem 2* are represented by blue-dashed dotted lines and red-dashed lines, respectively. The optimal solutions, represented by ‘•’ symbols, are obtained from minimizing $P_{\text{out}}(R_s)$ via an exhaustive search for different values of N_a . Similar as in Fig. 3, we first observe that the minimum secrecy outage probability $P_{\text{out}}^*(R_s)$ achieved by the beamformer solution from *Proposition 2* and *Theorem 2* is nearly the same as the optimal beamformer solution found through exhaustive search. We then observe that $P_{\text{out}}^*(R_s)$ decreases significantly as N_a decreases and $\tilde{\gamma}_{ab}$ increases. Moreover, we observe that the gap between the minimum $P_{\text{out}}(R_s)$ achieved by the beamformer solution from *Proposition 1* and *Theorem 1* and the minimum $P_{\text{out}}(R_s)$ achieved by the beamformer solution from *Proposition 2* and *Theorem 2* reduces as N_a increases, revealing that, in Rician wiretap channels with the jammer, the secrecy performance of the beamformer solution obtained from *Proposition 1* and *Theorem 1* (i.e., from **Algorithm 1**) is almost the same as the secrecy performance of the beamformer solution obtained from *Proposition 2* and *Theorem 2* when N_a is larger than 2.

In Fig. 6, we provide a schematic view of the optimal beamformer solutions for different values of K_{ae} . For illustration purpose, we denote \mathbf{w}^* as the optimal beamformer solution when J is not transmitting. We also denote \mathbf{w}_j^* as the optimal beamformer solution when J is transmitting. Fig. 6(a) shows the optimal beamformer solutions when $K_{ae} = 0$ (i.e., the Alice-Eve channel is in a pure Rayleigh fading environment). We see that \mathbf{w}^* and \mathbf{w}_j^* overlap with each other. We also see that \mathbf{w}^* and \mathbf{w}_j^* are in the same direction as the main channel \mathbf{h}_{ab} , indicating that the optimal beamformer solutions when $K_{ae} = 0$ are the maximal-ratio transmission such that the capacity of the main channel is maximized. Fig. 6(b) shows the optimal beamformer solutions when $K_{ae} = \infty$ (i.e., the Alice-Eve channel is in a pure LOS environment). We see that \mathbf{w}^* and \mathbf{w}_j^* overlap with \mathbf{w}_1 , revealing that the optimal beamformer solutions are orthogonal to the LOS component in the Alice-Eve channel \mathbf{G}_{ae}^o . Moreover, we

examine more general scenarios where K_{ae} is between the above two extremes. As a specific example, in Fig. 6(c) we show the optimal beamformer solutions of our scheme for $K_{ae} = 5$ dB. We first see that \mathbf{w}^* and \mathbf{w}_j^* are in different directions, which validates our analysis in *Theorem 2*. We then see that \mathbf{w}_j^* is closer to the main channel \mathbf{h}_{ab} , compared to \mathbf{w}^* . This is due to the fact that the jamming signals degrade the quality of the received signals at Eve.

We now examine the impact of the uncertainty in Eve's location. To this end, we adopt the time difference of arrival (TDOA) scheme discussed in [27] as the location estimation scheme. We then introduce the covariance matrix $\mathbf{V}_{pos} = \mathbf{J}^{-1}$, where \mathbf{J} denotes the Fisher matrix for TDOA scheme (see [27] for details). We further express \mathbf{V}_{pos} as

$$\mathbf{V}_{pos} = \begin{bmatrix} \sigma_x^2 & \sigma_{xy} \\ \sigma_{yx} & \sigma_y^2 \end{bmatrix}, \quad (54)$$

where the values of σ_x , σ_y , σ_{xy} , and σ_{yx} can be obtained straightforwardly from the inverse of \mathbf{J} . We denote Eve's true location as $\zeta_0 = [x_0, y_0]$, Eve's estimated location as $\zeta_e = [x_e, y_e]$, and the correlation coefficient as $\rho = \sigma_{xy} / (\sigma_x \sigma_y)$. As such, the distribution of Eve's estimated location can be expressed as

$$P(\zeta_e) = \frac{1}{2\pi\sqrt{1-\rho^2}\sigma_x\sigma_y} \exp \left\{ -\frac{1}{2(1-\rho^2)} \left(\frac{(x_e - x_0)^2}{\sigma_x^2} + \frac{(y_e - y_0)^2}{\sigma_y^2} - 2\rho \frac{(x_e - x_0)(y_e - y_0)}{\sigma_x\sigma_y} \right) \right\}. \quad (55)$$

In order to characterize the secrecy performance of the system, we adopt an "average" measure of $P_{out}(R_s)$, which is given by [27, Eq.(44)]

$$\bar{P}_{out}(R_s) = \int_{-\infty}^{\infty} \int_{-\infty}^{\infty} P_{out}(R_s) P(\xi_e) dx_e dy_e. \quad (56)$$

In Fig. 7, we plot $\bar{P}_{out}(R_s)$ versus τ for different levels of Eve's location uncertainty for both the case where \mathbf{J} is not transmitting and the case where \mathbf{J} is transmitting. In this figure, we adopt the TDOA scheme discussed in [27] as the location estimation scheme. In the TDOA scheme, the level of Eve's location uncertainty is represented by $c\sigma_t$, where c is the speed of the light, and σ_t is the standard deviation of the timings. The larger $c\sigma_t$ is, the less accurate Eve's location is. In this figure, we consider that Alice, Bob, and \mathbf{J} are located at [0 m, 0 m], [1225 m, 707 m], and [2000 m, -3464 m], respectively. We also consider that the true location of Eve is [1000 m, -1000 m]. We see that, for both cases, there exists a unique τ^* that minimizes $\bar{P}_{out}(R_s)$ for each $c\sigma_t$. We also see that the minimum $\bar{P}_{out}(R_s)$ increases as $c\sigma_t$ increases, which demonstrates that the secrecy performance of our scheme decreases, as the level of uncertainty in Eve's location increases. Although not completely shown here, we note that our results approach the appropriate solutions as the location uncertainty approaches both zero and infinity (i.e., location unknown), and show the expected trends between these two extremes. Moreover, compared to the case where \mathbf{J} is not transmitting, we can observe that, for a specific $c\sigma_t > 0$, the minimum $\bar{P}_{out}(R_s)$ of the case where \mathbf{J} is transmitting

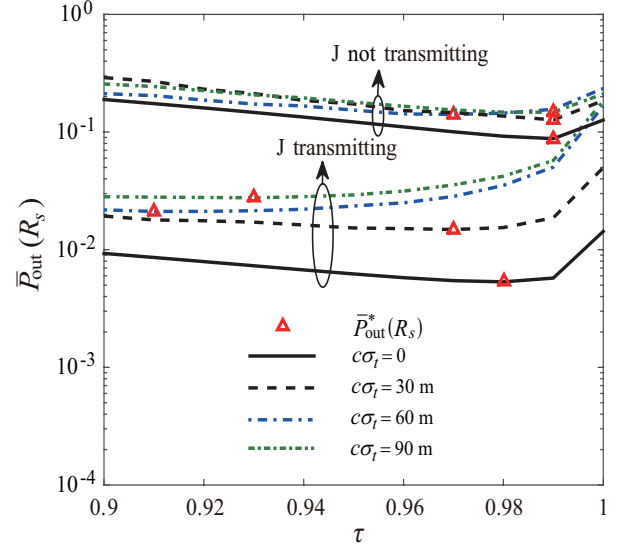


Fig. 7. $\bar{P}_{out}(R_s)$ versus τ for different values of $c\sigma_t$ with $N_a = 4$, $N_e = 2$, $N_j = 4$, $K_{ab} = 10$ dB, $K_{ae} = 5$ dB, $\tilde{\gamma}_{ab} = \tilde{\gamma}_{ae} = 10$ dB, $\theta_{ab} = \pi/3$, $\theta_{ae} = \pi/4$, and $R_s = 1$ bits/s/Hz.

is decreased (as expected). We note that similar trends and outcomes to those shown in Fig. 7 were found for a wide range of antenna configurations, transceiver locations, and Eve locations.

VI. CONCLUSION

In this work we have proposed a new LBB solution for Rician wiretap channels, in which a source communicates with a legitimate receiver in the presence of an eavesdropper. In our scheme, we assumed that the CSI from the legitimate receiver is known at the source, while the only available information on the eavesdropper at the source is her location. With no jammer present, we showed how the beamforming vector that minimizes the secrecy outage probability of the system can be obtained in real-time. We also examined the optimal beamformer solution in the presence of a multi-antenna jammer, showing how our real-time no-jammer solution still provides close-to-optimal performance in most practical scenarios. The work reported here illustrates how in a range of realistic wiretap channels, in which the only information known on an eavesdropper is her location, a real-time solution to the optimal beamformer can be determined and deployed.

APPENDIX A PROOF OF THEOREM 2

In order to derive the secrecy outage probability for Rician fading wiretap channels with a jammer for the special case of $K_{je} = 0$, we first need to derive the PDF of γ_e . We note that the closed-form expression for the PDF of γ_e is mathematically intractable due to the fact that γ_e is a random variable containing both the non-central complex normal vector $\mathbf{G}_{ae}\mathbf{w}$ and the random matrix \mathbf{R} . To address this problem, we consider the use of the gamma approximation to characterize the PDF of γ_e . Such an approximation has been

shown to be effective in accurately describing the distribution of the received SNR of Rician fading channels with Rayleigh-distributed co-channel interference [28]. As such, we express the gamma approximations of the PDF γ_e as

$$f_{\gamma_e}(x) = \frac{x^{\alpha-1} \exp\left(-\frac{x}{\beta}\right)}{\Gamma(\alpha) \beta^\alpha}, \quad (57)$$

where α denotes the scale parameter of the gamma distribution, and β denotes the shape parameter of the gamma distribution. We have $\alpha\beta$ and $\alpha\beta^2$ represent the mean and the variance of γ_e , respectively. We then express the CDF of γ_e as

$$F_{\gamma_e}(\gamma) = \frac{\gamma\left(\alpha, \frac{\gamma}{\beta}\right)}{\Gamma(\alpha)}, \quad (58)$$

We express the l th moment of γ_e as [29]

$$\xi_l = \tilde{\gamma}_{ae}^l \varphi_l \vartheta_l, \quad (59)$$

where φ_l and ϑ_l are as shown in (47) and (48), respectively. Based on (59), we obtain the mean of γ_e as

$$\mathbb{E}[\gamma_e] = \tilde{\gamma}_{ae} \varphi_1 \vartheta_1. \quad (60)$$

We then obtain the variance of γ_e as

$$\text{Var}(\gamma_e) = \tilde{\gamma}_{ae}^2 (\varphi_2 \vartheta_2 - \varphi_1^2 \vartheta_1^2). \quad (61)$$

From (60) and (61), we obtain α and β as

$$\alpha = \frac{\varphi_1^2 \vartheta_1^2}{\varphi_2 \vartheta_2 - \varphi_1^2 \vartheta_1^2}, \quad (62)$$

and

$$\beta = \tilde{\gamma}_{ae} \frac{(\varphi_2 \vartheta_2 - \varphi_1^2 \vartheta_1^2)}{\varphi_1 \vartheta_1}, \quad (63)$$

respectively.

We then re-express $P_{\text{out}}(R_s)$ in (21) as

$$\begin{aligned} P_{\text{out}}(R_s) &= \Pr(C_b - C_e < R_s | \gamma_b) \\ &= \Pr(C_e > C_b - R_s | \gamma_b) \\ &= \Pr(\gamma_e > 2^{-R_s} (1 + \gamma_b) - 1) \\ &= 1 - \int_0^{2^{-R_s} (1 + \gamma_b) - 1} f_{\gamma_e}(\gamma) d\gamma \\ &= 1 - F_{\gamma_e}(2^{-R_s} (1 + \gamma_b) - 1). \end{aligned} \quad (64)$$

Substituting (57), (58), (62), and (63) into (64), we obtain the desired result in (51). The proof is completed.

REFERENCES

- [1] N. Yang, L. Wang, G. Geraci, M. ElKashlan, J. Yuan, and M. Di Renzo, "Safeguarding 5G wireless communication networks using physical layer security," *IEEE Commun. Mag.*, vol. 53, no. 4, pp. 20–27, Apr. 2015.
- [2] A. Wyner, "The wire-tap channel," *Bell Syst. Tech. J.*, vol. 54, no. 8, pp. 1355–1387, Oct. 1975.
- [3] I. Csiszár and J. Körner, "Broadcast channels with confidential messages," *IEEE Trans. Inf. Theory*, vol. 24, no. 3, pp. 339–348, May 1978.
- [4] A. Khisti and G. W. Wornell, "Secure transmission with multiple antennas I: The MISOME wiretap channel," *IEEE Trans. Inf. Theory*, vol. 56, no. 6, pp. 3088–3104, Jul. 2010.
- [5] A. Khisti and G. W. Wornell, "Secure transmission with multiple antennas II: The MIMOME wiretap channel," *IEEE Trans. Inf. Theory*, vol. 56, no. 11, pp. 5515–5532, Nov. 2010.
- [6] C. Liu, G. Geraci, N. Yang, J. Yuan, and R. Malaney, "Beamforming for MIMO Gaussian channels with imperfect channel state information," in *Proc. IEEE Globecom 2013*, Atlanta, USA, Dec. 2013.
- [7] C. Liu, N. Yang, G. Geraci, J. Yuan, and R. Malaney, "Secrecy in MIMOME wiretap channels: Beamforming with imperfect CSI," in *Proc. IEEE ICC 2014*, Sydney, Australia, Jun. 2014.
- [8] N. Yang, G. Geraci, J. Yuan, and R. Malaney, "Confidential broadcasting via linear precoding in non-homogeneous MIMO multiuser networks," *IEEE Trans. Commun.*, vol. 62, no. 7, pp. 2515–2530, Jul. 2014.
- [9] J. Li, and A. P. Petropulu, "Ergodic secrecy rate for multiple-antenna wiretap channels with Rician fading," *IEEE Trans. Inf. Foren. Sec.*, vol. 6, no. 3, pp. 861–867, Sep. 2011.
- [10] X. Zhang, X. Zhou, and M. R. McKay, "On the design of artificial-noise-aided secure multi-antenna transmission in slow fading channels," *IEEE Trans. Veh. Technol.*, vol. 62, no. 5, pp. 2170–2181, Jun. 2013.
- [11] N. Yang, S. Yan, J. Yuan, R. Malaney, R. Subramanian, and I. Land, "Artificial noise: Transmission optimization in multi-input single-output wiretap channels," *IEEE Trans. Commun.*, vol. 63, no. 5, pp. 1771–1783, May 2015.
- [12] N. Yang, M. ElKashalan, T. Q. Duong, J. Yuan, and R. Malaney, "Optimal transmission with artificial noise in MISOME wiretap channels," *IEEE Trans. Veh. Technol.*, DOI: 10.1109/TVT.2015.2419318, 2015.
- [13] N. Yang, P. L. Yeoh, M. ElKashlan, R. Schober, and I. B. Collings, "Transmit antenna selection for security enhancement in MIMO wiretap channels," *IEEE Trans. Commun.*, vol. 61, no. 1, pp. 144–154, Jan. 2013.
- [14] N. Yang, P. L. Yeoh, M. ElKashlan, R. Schober, and J. Yuan, "MIMO wiretap channels: A secure transmission using transmit antenna selection and receive generalized selection combining," *IEEE Commun. Lett.*, vol. 17, no. 9, pp. 1754–1757, Sep. 2013.
- [15] S. Yan and R. Malaney, "Location-based beamforming for enhancing secrecy in Rician wiretap channels," arXiv:1412.6882, accepted by *IEEE Trans. Wireless Commun.*, 2015.
- [16] J. Wang, J. Lee, F. Wang, and T. Q. S. Quek, "Jamming-aided secure communication in massive MIMO Rician channels," *IEEE Trans. Wireless Commun.*, Vol. 14, No. 12, pp. 6854–6868, Dec. 2015.
- [17] J. -A. Tsai, R. Buehrer, and B. D. Woerner, "BER performance of a uniform circular array versus a uniform linear array in a mobile ratio environment," *IEEE Trans. Wireless Commun.*, vol. 3, no. 3, pp. 695–700, May 2004.
- [18] G. Taricco and E. Riegler, "On the ergodic capacity of correlated Rician fading MIMO channels with interference," *IEEE Trans. Inf. Theory*, vol. 57, no. 7, pp. 4123–4137, Jul. 2011.
- [19] C. Liu and R. Malaney, "Location-based beamforming for Rician wiretap channels," in *Proc. AusCTW 2016*, Melbourne, Australia, Jan. 2016.
- [20] F. Oggier and B. Hassibi, "The secrecy capacity of the MIMO wiretap channel," *IEEE Trans. Inf. Theory*, vol. 57, no. 8, pp. 4961–4972, Aug. 2011.
- [21] N. Kim, Y. Lee, and H. Park, "Performance analysis of MIMO system with linear MMSE receiver," *IEEE Trans. Wireless Commun.*, vol. 7, no. 11, pp. 4474–4478, Nov. 2008.
- [22] S. Gerbracht, C. Scheunert, and E. A. Jorswieck, "Secrecy outage in MISO systems with partial channel information," *IEEE Trans. Inf. Foren. Sec.*, vol. 7, no. 2, pp. 704–716, Apr. 2012.
- [23] I. S. Gradshteyn and I. M. Ryzhik, *Tabel of Integrals, Series, and Products*, 7th edition. Academic Press, 2007.
- [24] J. Borwein and P. Borwein, *Pi and the AGM: A Study in Analytic Number Theory and Computational Complexity*, John Wiley, 1987.
- [25] T. Andrews, "Computation time comparison between Matlab and C++ using launch windows," *Aerospace Engineering*, California Polytech State University: San Luis Obispo, pp. 1–6, Jun. 2012.
- [26] E. Perahia, A. Sheth, T. Kenney, R. Stacey, and D. Halperin, "Investigation into the Doppler component of the IEEE 802.11n channel model," in *Proc. IEEE Globecom 2010*, Miami, USA, Dec. 2010.
- [27] C. Liu, N. Yang, J. Yuan, and R. Malaney, "Location-based secure transmission for wiretap channels," *IEEE J. Sel. Areas Commun.*, vol. 33, no. 7, pp. 1458–1470, Jul. 2015.
- [28] R. H. Y. Louie, M. R. McKay, and I. B. Collings, "New performance results for multiuser optimum combining in the presence of Rician fading," *IEEE Trans. Commun.*, vol. 57, No. 8, pp. 2348–2358, Aug. 2009.
- [29] M. R. McKay, A. Zanella, I. B. Collings, and M. Chiani, "Error probability and SINR analysis of optimum combining in Rician fading," *IEEE Trans. Commun.*, vol. 57, no. 3, pp. 676–687, Mar. 2009.